Supporting information

Enzyme-Triggered Disassembly of Polymeric Micelles by Controlled Depolymerization via Cascade Cyclization for Anti-cancer Drug Delivery

Jaehyun Park[1, ‡], Seokhee Jo[2, ‡], Yeong Mi Lee[2], Gurusamy Saravanakumar[2,3], Junseok Lee[2,3], Dongsik Park[2], and Won Jong Kim[1, 2, 3, *]

[1]*School of Interdisciplinary Bioscience and Bioengineering, Pohang University of Science and Technology (POSTECH), Pohang 37673, South Korea.*

[2]*Department of Chemistry, POSTECH-CATHOLIC Biomedical Engineering Institute, POSTECH, Pohang 37673, South Korea.*

[3]*OmniaMed Co., Ltd, Pohang 37673, South Korea.*

[‡]These authors contributed equally to this work.

[*]Corresponding author: Won Jong Kim, Ph. D. (e-mail: wjkim@postech.ac.kr)

(a)

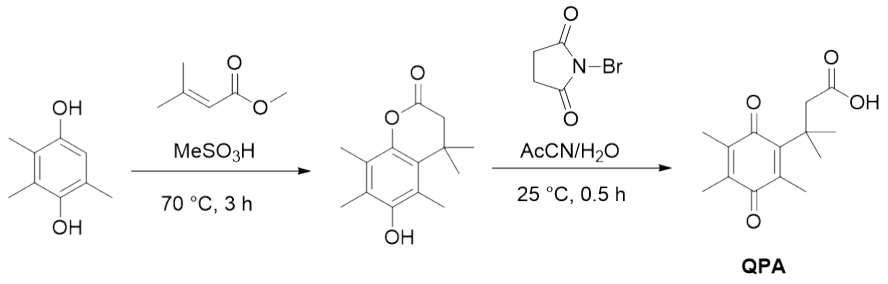

(b)

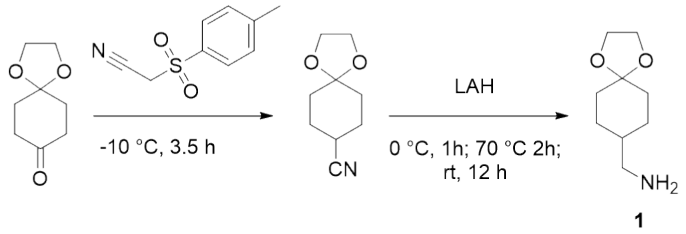

Scheme S1. Synthesis of (a) carboxylic acid functionalized QPA trigger moiety and (b) precursor compound 4-(aminomethyl)cyclohexanone ethylene ketal (1).

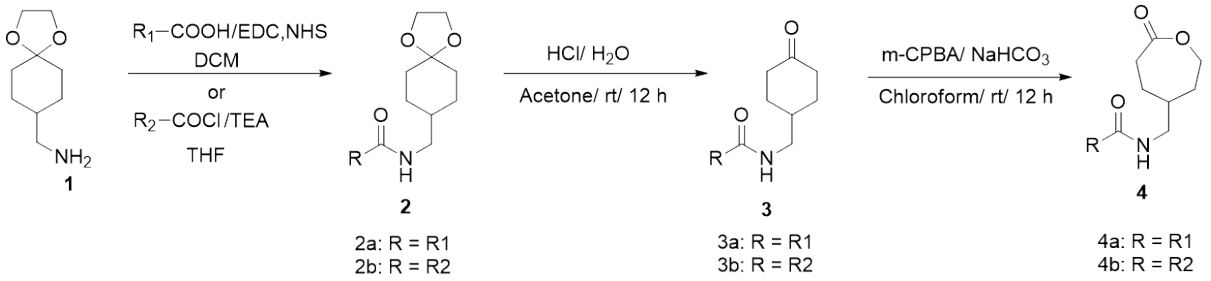

Scheme S2. Reaction scheme for the synthesis of enzyme-responsive (γ-QPA-ε-CL, 4a) and control caprolactone monomer (γ-Bz-ε-CL, 4b).

Table S1. Properties of diblock copolymers.

Polymer	Composition[a]	M_n, NMR (kDa)[a]	M_n, GPC (kDa)[b]	M_w/M_n[b]
QPA-P	PEG_{45}-*b*-$(PCL\text{-}QPA)_{2.22}$	2.83	2.80	1.23
Bz-P	PEG_{45}-*b*-$(PCL\text{-}Bz)_{2.44}$	2.60	2.67	1.15

[a]The compositions of copolymers are calculated from ^{1}H NMR in $CDCl_3$, [b]Determined by GPC.

Table S2. Characteristics of blank and DOX loaded QPA-PM and Bz-PM.

Micelles	Feed (wt.%)	DLC (wt.%)	DLE (%)	Size (nm)[a]	PDI[a]
QPA-PM-DOX	20	5.67±1.16	28.3±5.8	25.29±2.8	0.278±0.011
Bz-PM-DOX	20	4.81±0.76	24.0±3.8	23.0±0.7	0.295±0.015

[a]Determined using DLS at 25 °C in distilled water.

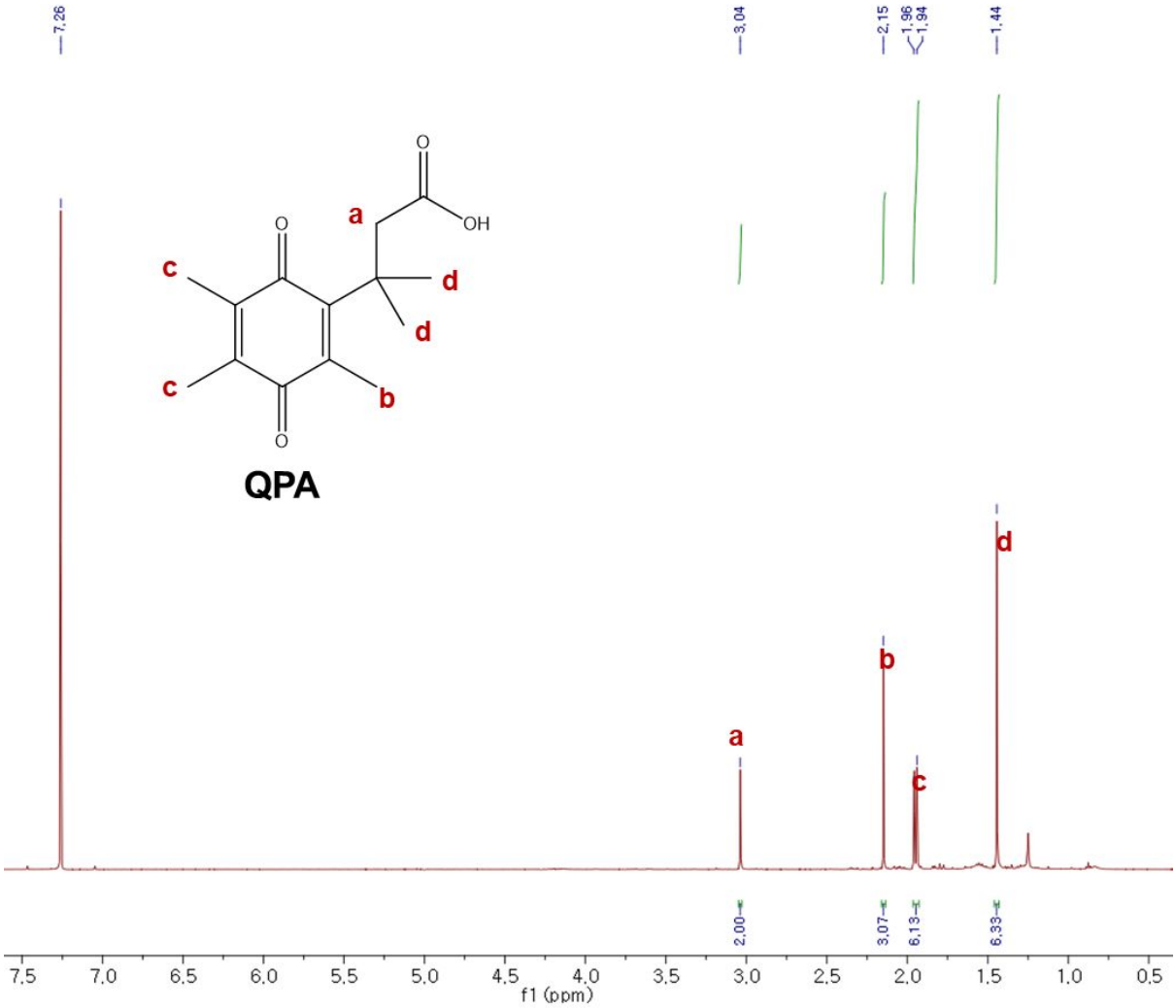

Figure S1. ^{1}H-NMR spectrum of quinone propionic acid (QPA) in $CDCl_3$

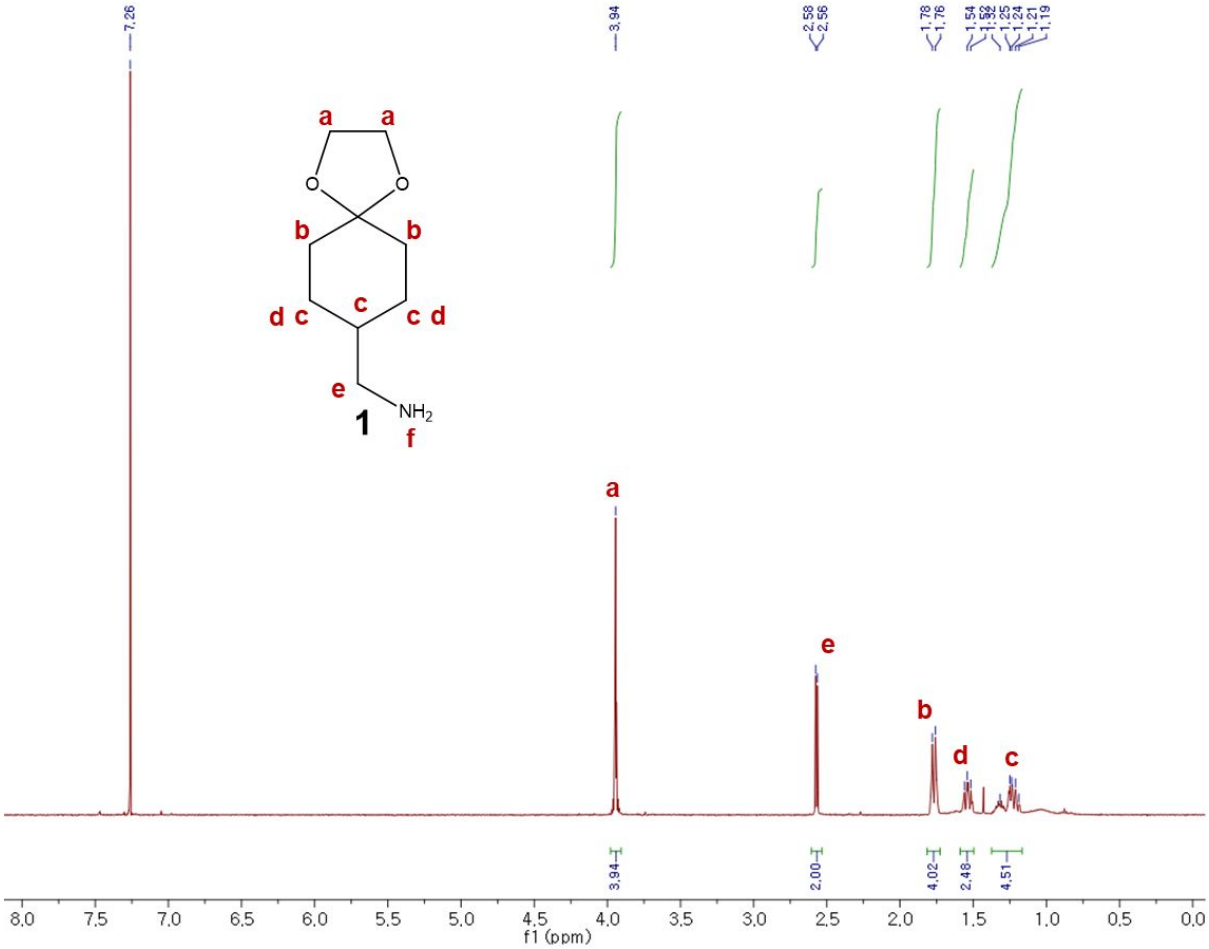

Figure S2. ^{1}H-NMR spectrum of acetal-methylamine (Compound 1) in $CDCl_3$.

(a)

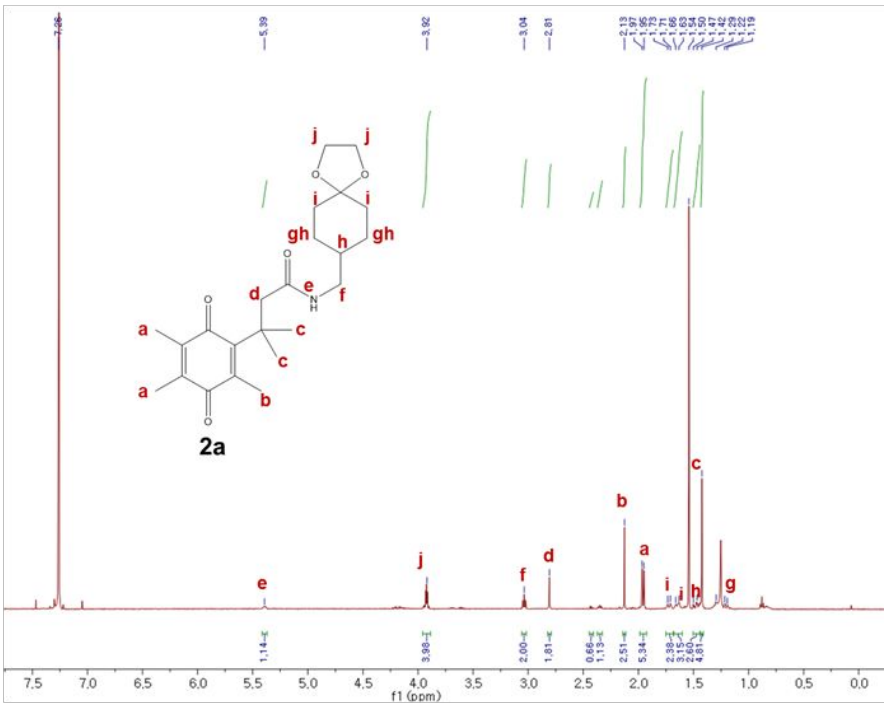

(b)

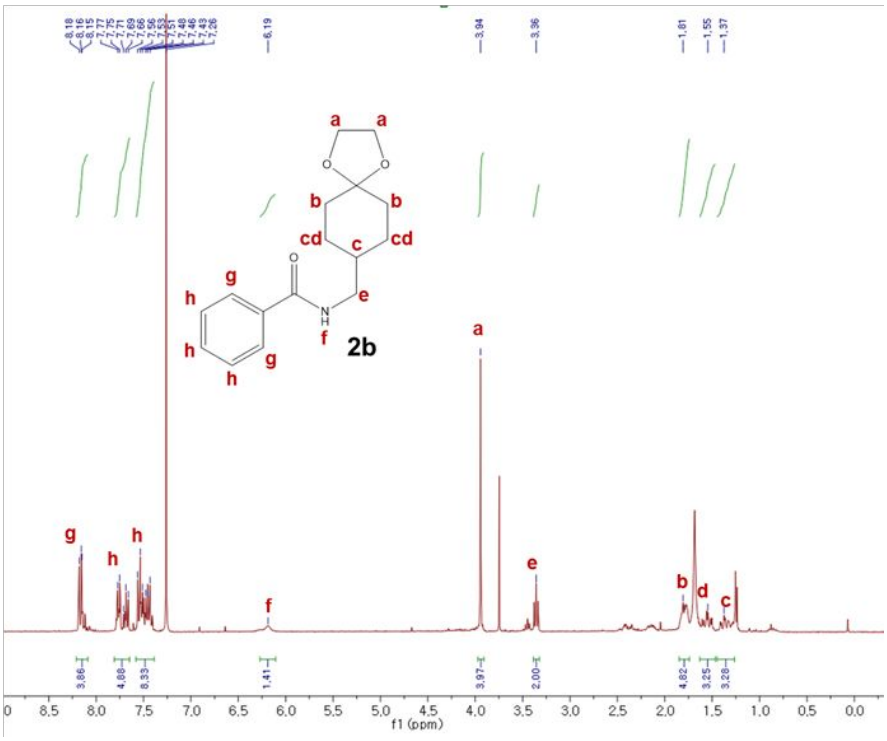

Figure S3. ^{1}H-NMR spectrum of (a) acetal-QPA (Compound 2a) and (b) acetal-Bz (Compound 2b) in $CDCl_3$

(a)

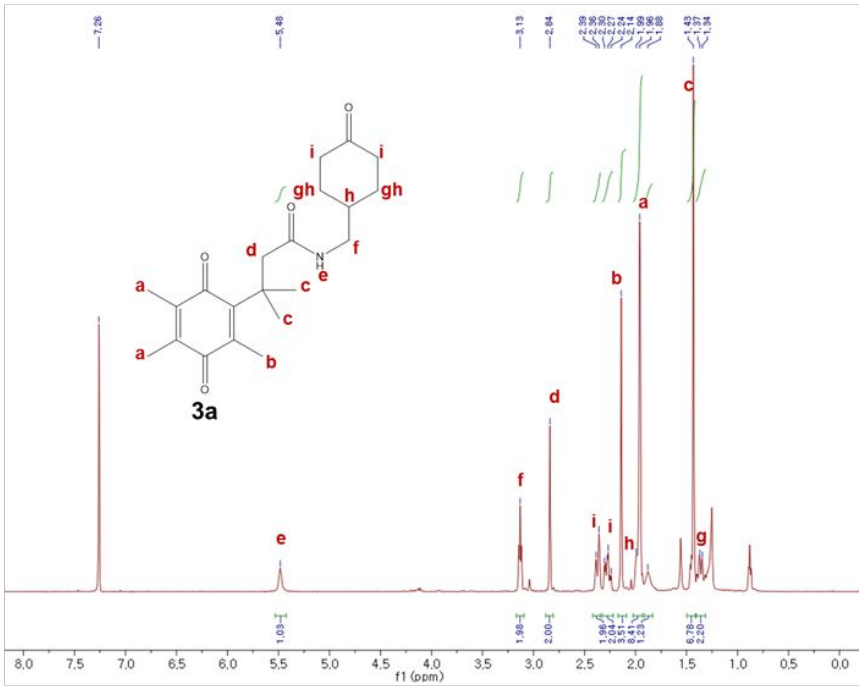

(b)

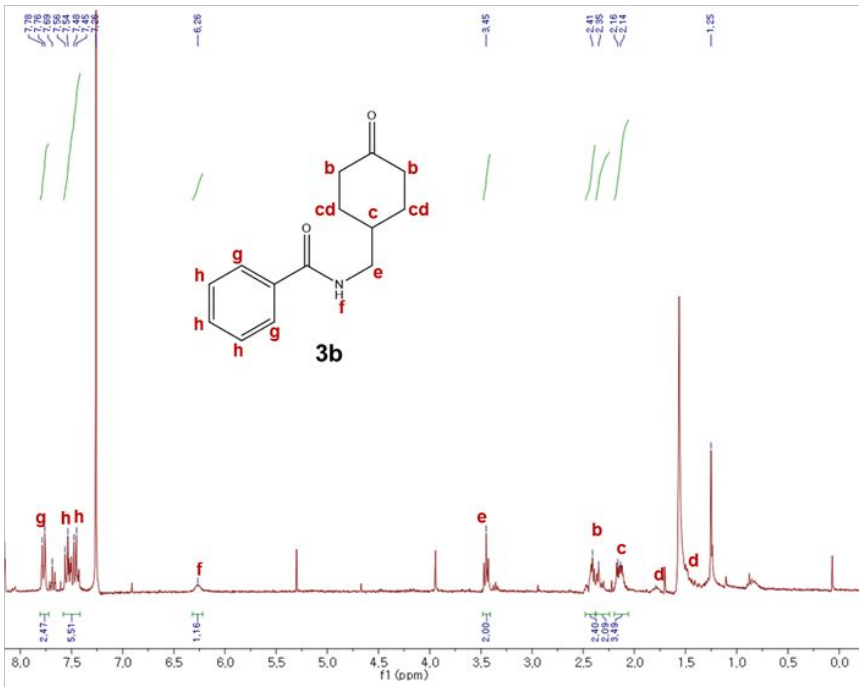

Figure S4. ^{1}H-NMR spectrum of (a) ketone-QPA (Compound 3a) and (b) acetal-Bz (Compound 3b) in $CDCl_3$.

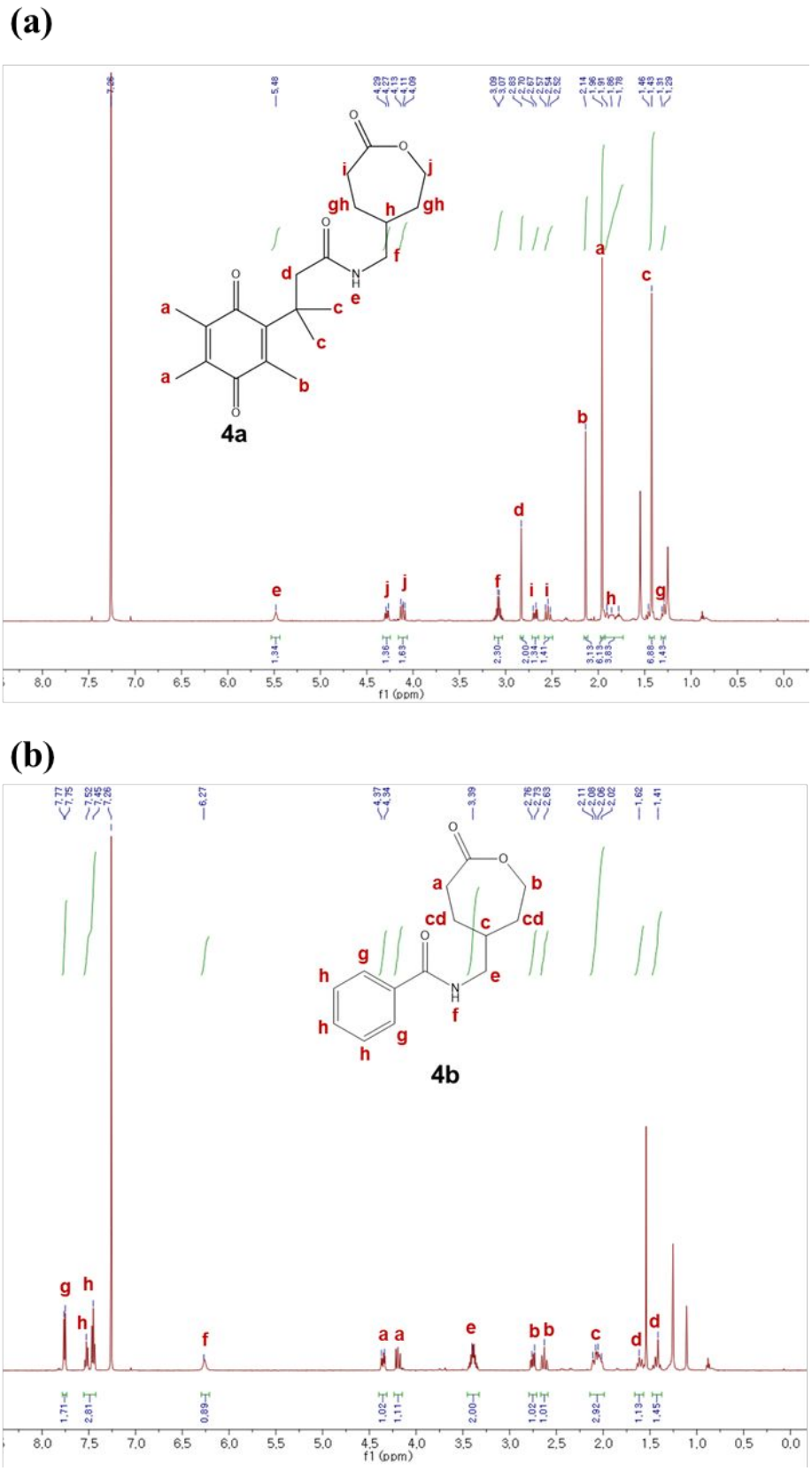

Figure S5. ^{1}H-NMR spectrum of (a) ester-QPA (Compound 4a) and (b) ester-Bz (Compound 4b) in $CDCl_3$

(a)

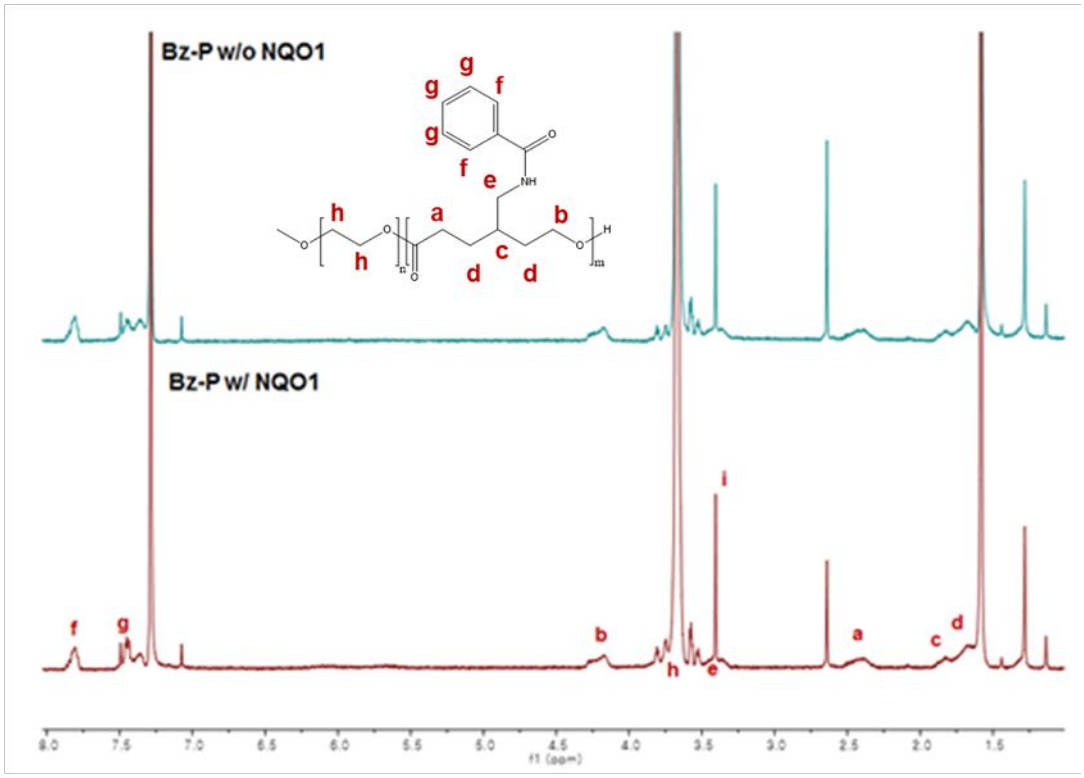

(b)

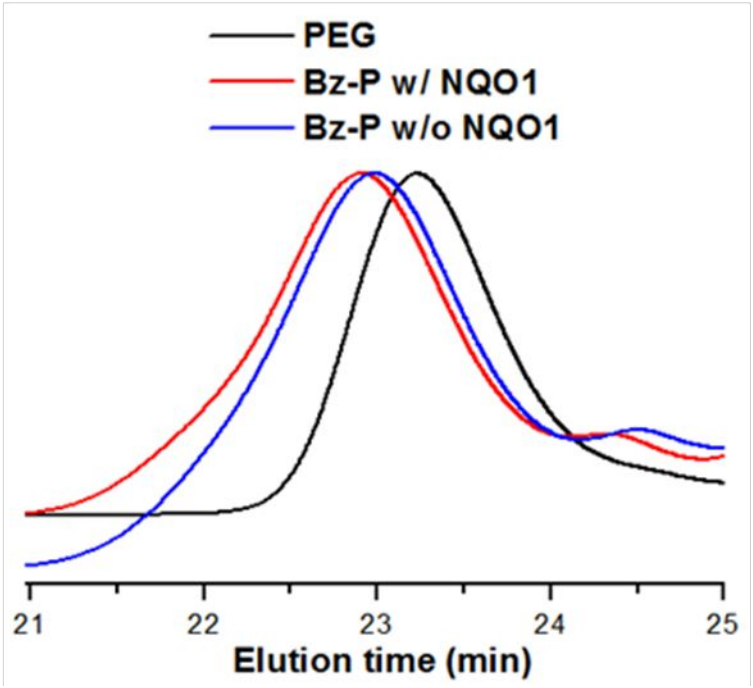

Figure S6. (a) ^{1}H-NMR and (b) GPC profiles of Bz-P before and after incubation with NQO1.

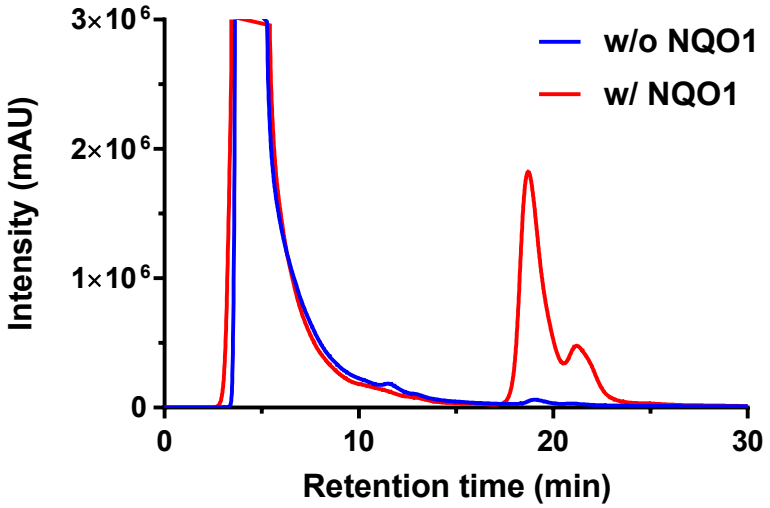

Figure S7. HPLC chromatogram of QPA-P before and after incubation with NQO1.

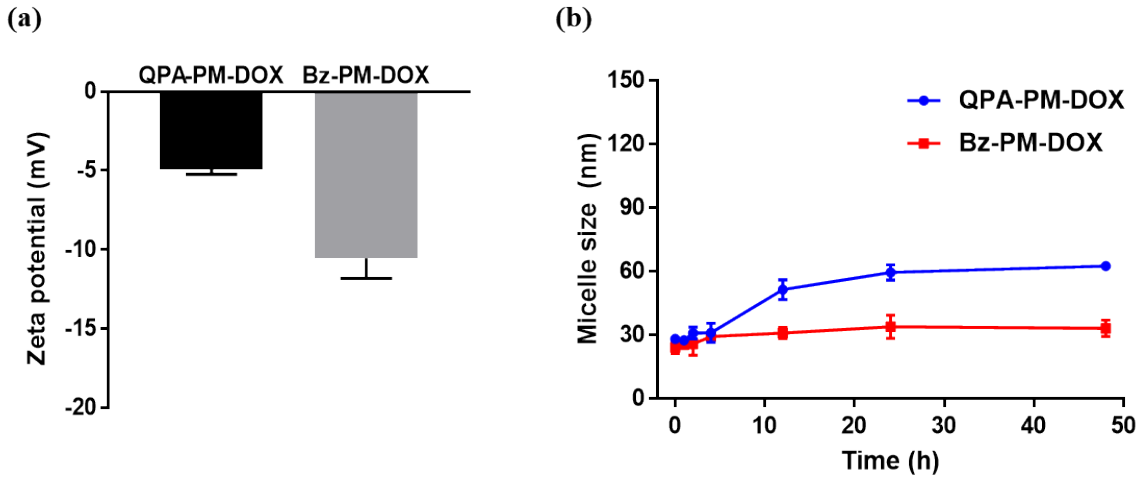

Figure S8. (a) Zeta potential and (b) Serum stability of QPA-PM-DOX and Bz-PM-DOX.

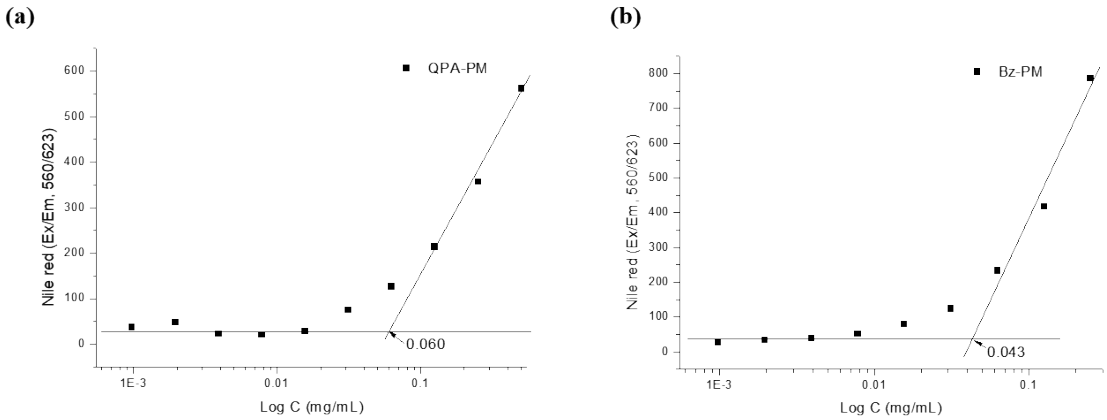

Figure S9. Critical micellar concentration (CMC) of (a) QPA-PM and (b) Bz-PM.

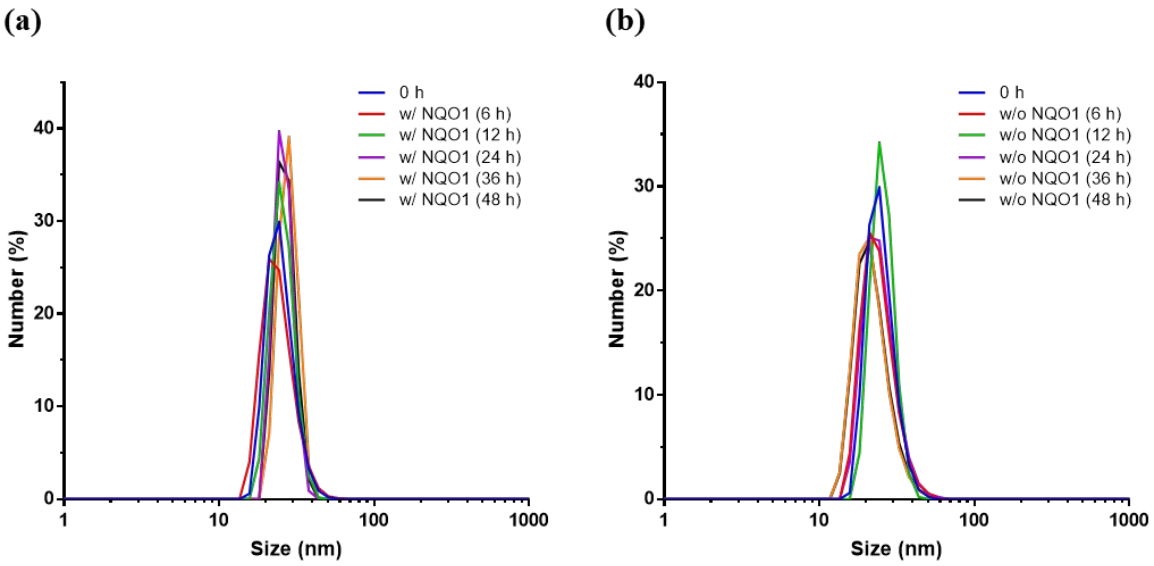

Figure S10. Change in particle size distribution of (a) QPA-PM and (b) Bz-PM without enzyme NQO1.

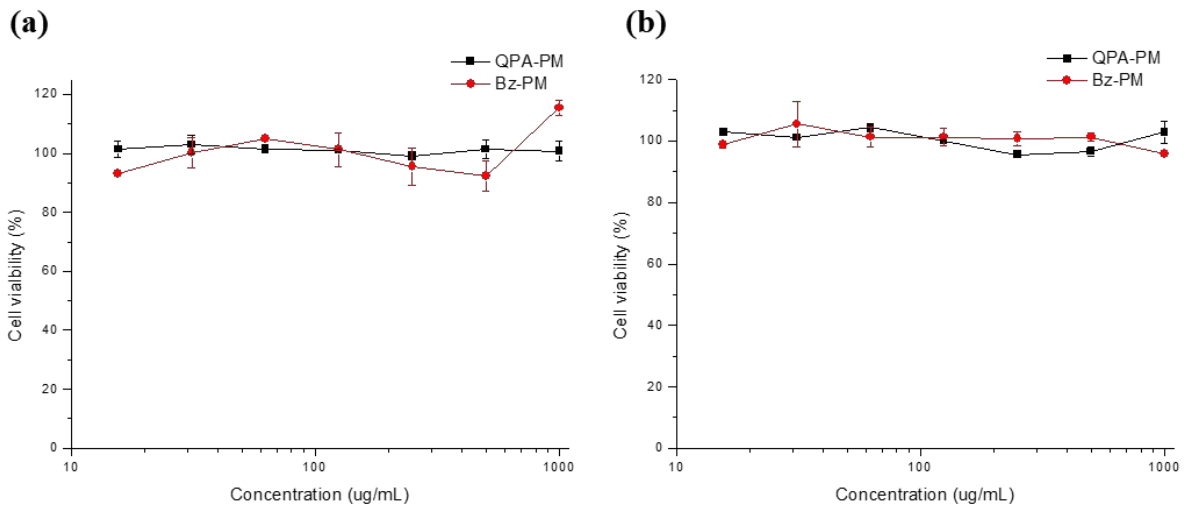

Figure S11. *In vitro* cytotoxicity of DOX-free micelles on (a) A549 and (b) H596 cell lines.

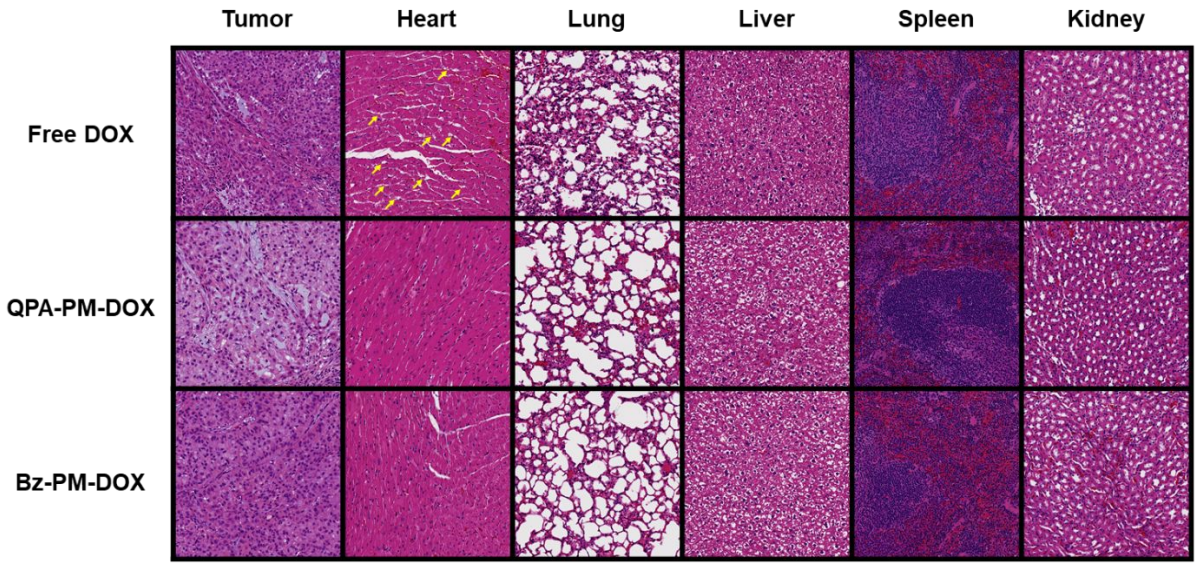

Figure S12. Histological evaluation of major organs after treatment of free DOX and DOX-loaded micelles. Vacuolization in heart tissue was depicted by yellow arrows.